Hydraulicity of lime plasters from Teotihuacan (Mexico): a microchemical and microphysical approach

Domenico Miriello[1], Luis Barba Pingarrón [2], Arturo Barba Pingarrón[3], Donatella Barca[1], Andrea Bloise[1], Jesús Rafael González Parra[3], Gino Mirocle Crisci[1], Raffaella De Luca[1*], Genea Girimonte[4], Jose Luis Ruvalcaba-Sil[5], Alessandra Pecci[4]

[1] Università della Calabria, Dipartimento di Biologia, Ecologia e Scienze della Terra, Arcavacata di Rende, Italy.

[2] Universidad Nacional Autónoma de México, Instituto de Investigaciones Antropológicas, México.

[3] Centro de Ingeniería de Superficies y Acabados (CENISA), Departamento de Ingeniería de Diseño y Manufactura, División de Ingeniería Mecánica e Industrial, Facultad de Ingeniería, Ciudad de México.

[4] Universitat de Barcelona, ERAAUB Research Group, Department of History and Archaeology, Barcelona, Spain.

[5] Universidad Nacional Autónoma de México, Instituto de Física, Ciudad de Mexico.

* Corresponding author: raffaella.deluca@unical.it

ABSTRACT

In this paper, results obtained from the compositional characterization of 11 samples of plaster, originating from the Teotihuacan archaeological area (Mexico), have been presented. Teotihuacan plasters are generally made of two layers, with the outermost layer, locally called *enlucido*, composed of a mixture of lime and volcanic glass shards; and the underlying layer, locally called *firme*, consisting of crushed volcanic scoria (defined locally as *tezontle*) mixed with a mud-based binder. Our first hypothesis was that the presence of glass shards would produce hydraulicity in the plasters. However, the combination of microchemical (energy dispersive spectrometer (EDS) microchemical analysis), microphysical (Vickers microhardness) and petrographic (optical microscopy) measurements made it possible to definitively clarify that this significant external plaster layer hardness was essentially due to the reactivity of the *tezontle*, which makes it hydraulic. Portable X-ray fluorescence analysis was also performed on the pigmented areas of the plasters, confirming that the red and green pigments, which are common pigments in pre-Columbian Teotihuacan, were mainly made from hematite and malachite, respectively.

Keywords:

Plasters

Glass shards

Tezontle volcanic scoria

Microhardness

C-S-H compounds

Mesoamerica

Teotihuacan

1. Introduction

Teotihuacan, which is considered to be one of the most important ancient Mesoamerican cities, lies approximately 50 km north of Mexico City (Fig. 1a). It was a powerful city, whose cultural, religious, and commercial influence extended far beyond its borders (Cowgill, 2015; Manzanilla, 2009, 2015). Teotihuacan (0–550 AD) is well known for its large pyramids (the Sun and the Moon pyramids) and occupies more than 20 km² in a plain surrounded by mountains and volcanoes: the valley of Teotihuacan. Archaeological research has revealed that the city was divided into four quadrants, quasi-oriented towards the four cardinal points. There were more than two thousand compounds (buildings that served as apartment compounds, neighbourhood centres, or that had other civil or ritual functions (Millon, 1973; Manzanilla, 2009)), where most of the population was concentrated. These compounds had different building phases, and most of them were covered in a lime plaster (Barba et al., 2009; Murakami, 2010, 2016).

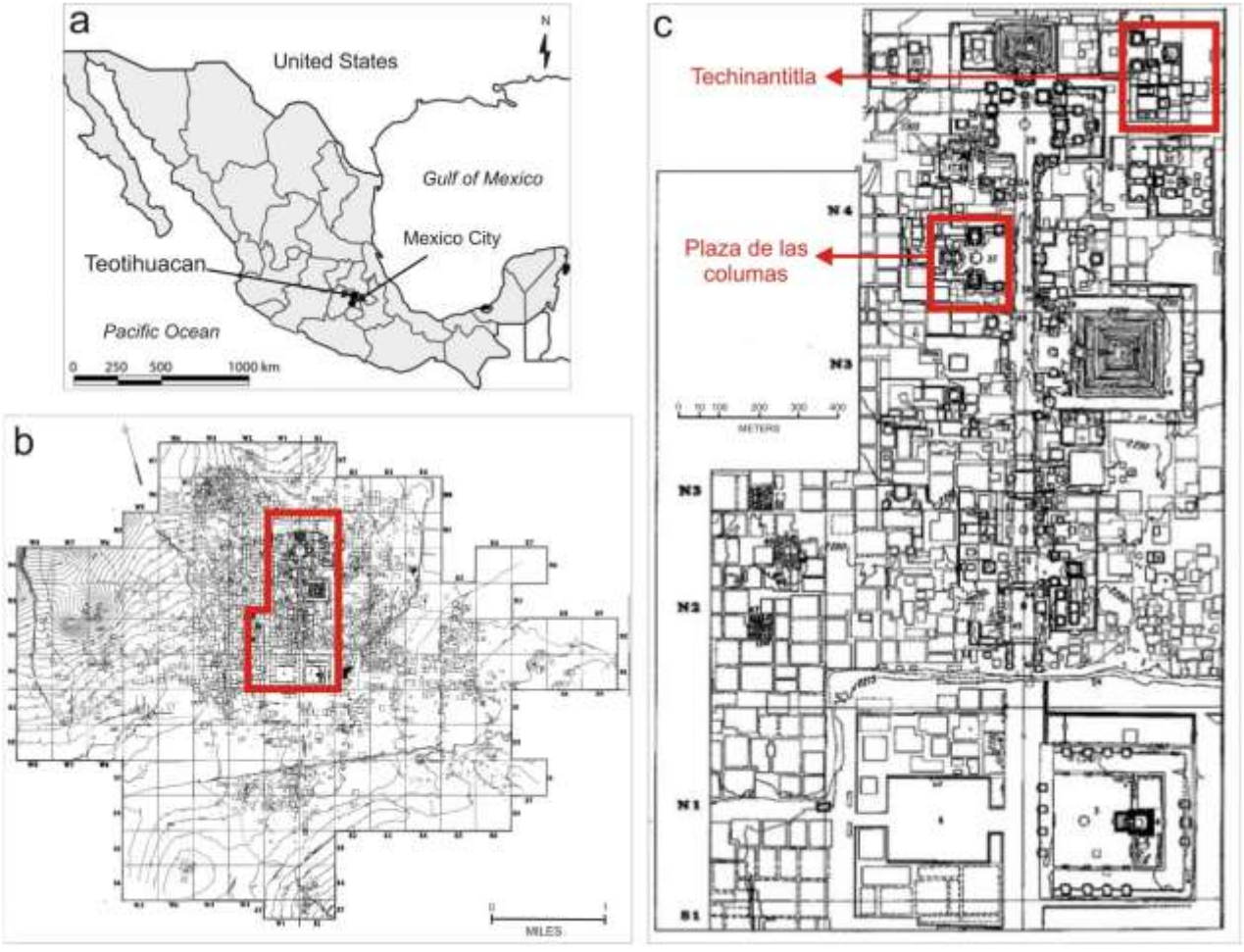

Fig. 1. a) Location of Teotihuacan, Mexico; **b)** Map of Teotihuacan (from Millon 1973); **c)** Inset map showing locations of the Techinantitla and Plaza de las Columnas study areas.

It has been found that Teotihuacan plasters are generally composed of two layers (Barba et al., 2009): a lower layer, called *firme* (Fig. 2a), consisting of crushed volcanic scoria (defined as *tezontle*) mixed with a mud-based binder, and a thin superficial layer called "*enlucido*" (Fig. 2a), based on lime mixed with glass shards (Fig. 2b). The *enlucido* generally has low porosity and appears homogeneous when viewed macroscopically. This layer is generally compact, and the aggregate cannot be distinguished with the naked eye; it was used in the same way for floors, walls and mural paintings, where pigmented layers had also been applied (De La Fuente, 1996; Magaloni, 1996; Marquina, 1922).

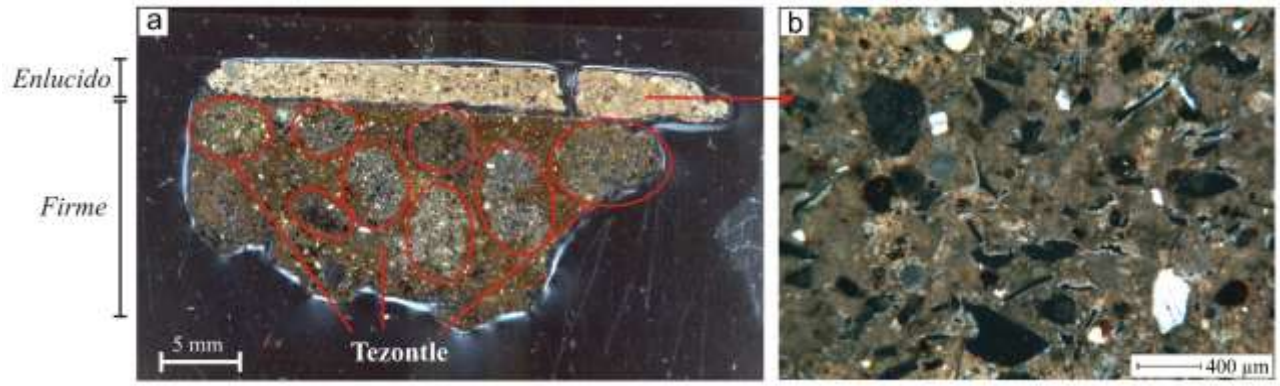

Fig. 2. a) Thin section of sample 53, under crossed nicol, with indication of the *enlucido* (outer) and *firme* (inner) layers and the presence of *tezontle* fragments; **b)** Microphotographs of sample 53 in thin section, taken using optical microscopy under crossed nicol, with the detail of the *enlucido* layer including its glass shards.

Previous studies (Pecci et al., 2018a, 2018b) on one of Teotihuacan's neighbourhoods (Teopancazco)—which was excavated by Dr Manzanilla over more than a decade ago (Manzanilla, 2012, 2015, 2018)—have shown that no changes occurred to this plaster preparation method for over four centuries. This allowed us to consider the presence of a technological style in their manufacture, which was characterized by producing plaster by mixing lime with volcanic glass shards. In the case of Teopancazco, the shards were sourced from the Altotonga (Veracruz) magmatic system (Barca et al., 2013, 2019; Pecci et al., 2018a, 2018b; Barba et al., 2019), suggesting that this style was originally developed in Teopancazco and later introduced throughout Teotihuacan. Plasters from Xalla, an important compound of Teotihuacan, were also made mixing lime and glass shards from Altotonga (Veracruz) magmatic system (Barca et al., 2019).

Murakami (2010) recorded the presence of glass shards in the plasters of different compounds in Teotihuacan from the early Xolalpan phase (AD 350). While looking at Magaloni micrographs published in 1996, it is possible to recognise that glass shards (and not quartz as she mentions) were incorporated into Teotihuacan murals during phase II of the Teotihuacan Pictorial period (Magaloni, 1996), in the early Tlamililolpa phase, and remained in use until the last phase, in the Metepec period. For these Teotihuacan buildings, the provenance of the glass shards has not been studied, yet, and remains unknown.

It is important to mention that the combination of *firme* and *enlucido* was very successful in Teotihuacan because the common presence of clayish soils there allowed a large volume of this material to be used as mud mortar for wall construction. Moreover, clayish soils were mixed with *tezontle* to produce the *concreto teotihuacano*, which was very useful for smoothing the surface and providing a solid *firme*—to which lime plaster was applied for waterproofing. This combination allowed the builders to save a lot of materials and energy because lime was not available in Teotihuacan, and we know that it came from outcrops near Tula (which is located in the city of Tula de Allende in the Tula Valley, in what is now the SW of the Mexican state of Hidalgo, NW of Mexico City).

Studying ancient mortars and plasters helps to both clarify the construction history of ancient buildings (Miriello et al., 2010; De Luca et al., 2013) and also to obtain data that can be used to recreate compatible mortars and plasters during restoration processes (Miriello et al., 2013). In the study described in this paper, after having characterized plaster samples from two Teotihuacan buildings and analysed the main pigments used in some of the paints, we concentrated on studying the hydraulic characteristics of the plasters. Our testing allowed us to definitively clarify an issue that has been open for some time—that is, whether or not the plasters of Teotihuacan were hydraulic, and if they were, which compositional features made them so.

As a matter of fact, the outer *enlucido* of the Teotihuacan plasters has demonstrated extraordinary hardness, even if it is very thin compared to the lower *firme*. This hardness could be due to hydraulic reactions between volcanic materials (glass shards and / or *tezontle*) and lime, which could cause the formation of C-S-H compounds (Taylor, 1997; Miriello et al., 2017) with low crystallinity, which are hardly detectable by X-ray diffraction (XRD).

Our initial hypothesis was that the hydraulic reactions were produced by the presence of the glass shards (rhyolitic glass), which comprise the majority of the *enlucido* aggregate. However, the problem was much more complex than it looked, and our first data contradicted this hypothesis.

The main aim of the work described in this paper was therefore to understand whether the hydraulicity of the *enlucido* was due to the reactivity of the glass shards, the reactivity of the *tezontle* (which is present in the *firme*), the initial composition of the limestone used to produce the lime, or a combination of these factors. To do this, microchemical (microchemical energy-dispersive X-ray spectroscopy (EDS) analysis) and microphysical (microhardness) approaches were used, coupled with polarized light-transmitted optical microscopy (OM).

Some samples, partially painted in red and green, were also studied using a portable X-ray fluorescence system (p-XRF) developed by the Instituto de Física of the Universidad Nacional Autónoma de México (UNAM; Ruvalcaba et al., 2010) to identify the pigments.

Samples for analysis came from two buildings located in the city of Teotihuacan, which have been referred to by Teotihuacan archaeologists as the Techinantitla and the Plaza de las Columnas compounds (Fig. 1c). Techinantitla is a single, very large compound (at least 75 × 95 m) located to the east of the Moon Pyramid

(Cabrera, 1996; De La Fuente, 1996). Its size makes it one of the largest compounds known at Teotihuacan (Manzanilla, 2009; Millon, 1973). It is possible that it was not a residential compound but rather a public, or semi-public building. The area of the compound is also known as the Barrio of the Looted Murals. In fact, René Millon was able to identify it as the origin of most of the looted murals, later donated by Wagner to The Young Memorial Museum of San Francisco (Muñoz Fuentes, 2019).

The Plaza de las Columnas compound is located to the west of the Street of the Dead (Calle de los Muertos), the main avenue of Teotihuacan, on the opposite side of the Pyramid of the Sun, in an area located between the Moon and the Sun pyramids. Archaeological research projects have recently been carried out at both sites, by the Proyecto Plaza de las Columnas, directed by Saburo Sugiyama, in collaboration with the UNAM.

2. Sampling and analytical techniques

2.1 Materials

Eleven plaster samples were analysed in this study (Fig. 3; Table 1). They were all wall or floor fragments and came from two specific sites inside the Teotihuacan archaeological area—seven from the Techinantitla compound (samples 60B, 60C, 61A, 61B, 61C, 5A, and 5B – Fig. 3a), and four from the Plaza de las Columnas compound (51A, 52A, 52B and 53 – Fig. 3b). All the samples were recovered from the surface during archaeological prospections at the two sites; hence, their precise original locations remain unknown. Some of the samples were clearly mural fragments (60B, 60C, 61A, 61C, and 52A), while others could belong to either floors or walls (5A, 5B, 61B, 51A, 52B, and 52B) (Fig. 3). The presence of clay materials in their inner layers (*firme*) makes this layer very brittle and difficult to preserve after sampling, to the extent that only samples 5B, 53, 60C and 61A still had the *firme* layer when they were prepared for thin section (Table 2).

In any case, this was not of great importance because the objective of this study was not to clarify the construction phases of the two sites, but to understand if Teotihuacan plasters were hydraulic, and, if so, where this hydraulicity came from. Moreover, we wanted to show that the study of plasters could provide important information on the technology of ancient cultures, even if the samples' specific archaeological provenances is not precisely known.

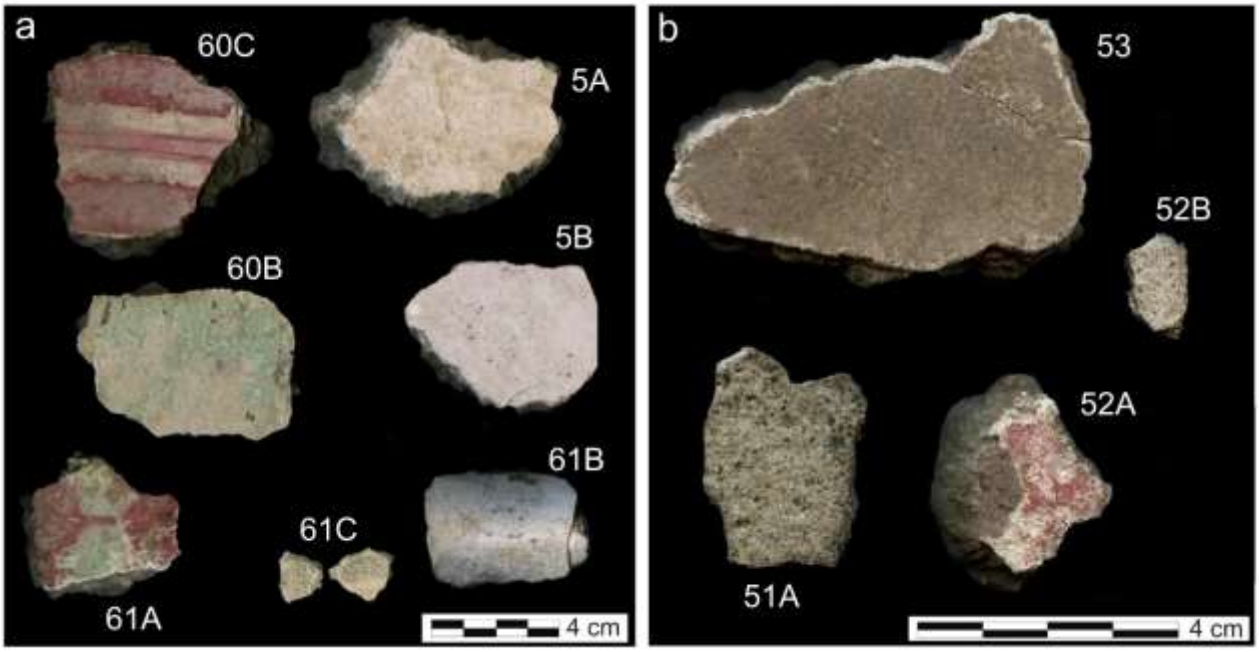

Fig. 3. Macroscopic aspect of the 11 plaster fragments studied showing those taken from **a)** Techinantitla and **b)** Plaza de las Columnas.

Sample	Location	Typology and macroscopic description
5A	Techinantitla	Plaster with a thick layer of white enlucido
5B	Techinantitla	Plaster with a thick layer of white enlucido
51A	Plaza de las Columnas	Plaster with only enlucido
52A	Plaza de las Columnas	Plaster with a thick layer of enlucido with a red pigmentation
52B	Plaza de las Columnas	Plaster with only enlucido
53	Plaza de las Columnas	Plaster with a thick layer of enlucido
60B	Techinantitla	Plaster with a thin layer of enlucido with a green pigmentation and traces of red
60C	Techinantitla	Plaster with a thin layer of enlucido with a red pigmentation
61A	Techinantitla	Plaster with a green and red pigmentation
61B	Techinantitla	Plaster with an enlucido of rounded profile, probably a wall/floor corner (chaflan)
61C	Techinantitla	Plaster with only enlucido

Table 1. Locations, typologies, and short macroscopic descriptions for Teotihuacan samples.

2.2 Methods

Petrographic analysis was performed using a Zeiss-Axioskop 40 microscope coupled with a Canon PowerShot A640 camera for polarized light microscopy (Table 2). Aggregate sorting divisions were defined by qualitative visual estimation charts using textural comparators for the degree of sorting in 2-D (Boggs, 2010; Jerram, 2001). Semi-quantitative estimates of the percentages of binder and aggregate, as volume fractions, and of macroporosity (d > 1/16 mm), were also obtained by comparing thin sections (as observed by optical

microscopy) with visual charts to support estimation of modal proportions of the minerals present in the rocks (Ricci Lucchi 1980; Myron Best 2003).

Microhardness was determined using a digital micro Vickers hardness tester (model HVS-1000) at the UNAM Center of Surface Engineering and Finishing (CENISA) Engineering Lab. This tool consisted of an arm on which 100 x and 400 x magnification objectives were mounted together with a diamond point that constituted the point that transmitted the load, which could be varied through the range of 10–1000 g. This tool allowed us to select the optimal analysis parameters for each sample. In our work, we chose to carry out the survey always using the same conditions, so that we could compare the results obtained according to the following formula:

Force = 0.2452 N / 0.025 kg; time = 15 s

Material microhardness calculations (Table 3) were performed using geometric measurements, which took advantage of the length of the diagonals of the impression left by the tip of the instrument on the material. Once we had established the time and charge parameters, we chose to proceed using a grid made up of three lines on each sample, each of which was comprised of five analysis points along a horizontal axis. All measuring points were taken at a distance of approximately 300 μm from each other. We performed this procedure successfully on all the samples, with the exceptions of 53 and 5B, whose materials were insufficient to carry out the microhardness measuring process.

We performed p-XRF analyses on the painted surfaces at the Instituto de Física, UNAM, using a portable system (SANDRA; Ruvalcaba et al., 2010). This system has a typical geometric configuration, and the AmpTek SDD detector was set at 45° from the direction of the excitation X-rays. The available X-ray tubes (XTF5011 model; Oxford Instruments) had Mo, Rh, and W anodes with a 125 μm beryllium window. The maximum power of the X-ray tubes was 75 W (50 kV, 1.5 mA), and the X-ray tube was powered by a high-voltage power supply (model XLG50P100; Spellman). The beam spot on the material surface was 1 mm, and the X-ray tube was mounted on an X–Y–Z support, so that it could be manually moved 3 cm in each direction in front of the studied object; thus, the region selected for analysis could be reached easily (Ruvalcaba et al., 2010). The points chosen on each sample for analysis using the Mo X-ray tube can be seen in Fig. 5, in which "R" points were those analysed on the red pigment, "G" indicates points taken on the green pigment, and "W" indicates not-pigmented plaster.

Microchemical binder analyses were performed to highlight any reaction between the volcanic materials and the binder (Tables 4 and 5). These analyses were carried out using an electron probe micro-analysis (EPMA; model JEOL-JXA 8230) coupled with a spectrometer EDS (model JEOL EX-94310FaL1Q) and five WDS spectrometers (XCE types) equipped with LDE, TAP, LIF, and PETJ crystals. EPMA / WDS single-point analyses were performed using a 15 kV accelerating voltage, a 10 nA probe current, and counting times of 30 s for elemental peaks, and 5 s for backgrounds. Element X-ray mapping was performed with a WDS system using a 50.0 nA probe current, 15 keV accelerating voltage, and 15 ms dwell time. A set of standards (Ref. # 02757-

AB; SPI Supplies, Metals & Minerals Standard, serial 4AK) containing minerals with declared compositions was used for quantification. WDS microanalysis was carried out using the standardless ZAF correction method. All samples were polished and carbon coated with graphite using a Quorum Q150T ES sputter coater. All of the SEM / EDS and EPMA analyses were performed at the "Laboratorio di Microscopia Elettronica e Microanalisi (CM2)", University of Calabria, Italy (UNICAL).

3. Results and discussion

3.1. Petrographic and mineralogical features of the plasters

As mentioned above, the Teotihuacan plaster samples are generally made in two layers (Fig. 2a), with the *enlucido* (top, or finishing layer) composed of lime mixed with glass shards (Fig. 2b), and generally very thin, seldom exceeding 10 mm (Barba et al., 2009; Barca et al., 2013, 2019). This layer has been found in plasters from the Teopancazco compound since the Early Tlamimilolpa phase, and in other compounds in Teotihuacan only since the early Xolalpan phase (AD 350) (Murakami, 2010; Pecci et al., 2018a). The second, *firme* layer, consists of crushed volcanic scoria (locally *tezontle*) mixed with a mud-based binder (Fig. 2a).

In some samples (5A, 53 and 61A), there were two outer layers of *enlucido* (Fig. 4a and Table 2). The presence of two or more *enlucido* layers in pre-Columbian plasters can be explained as re-plastering. This construction practice has been discussed in the work of Miriello et al. (2015) and had already been highlighted in ancient plasters from Teotihuacan by Pecci et al. (2018a) and in Mayan plasters by Villaseñor et al. (2009).

All the analysed samples were characterized by the presence of abundant glass shards in the *enlucido* (Fig. 4b), except for sample 51A (Fig. 4c), where they were present only as traces. Published data (De La Fuente, 1996; Murakami, 2010; Pecci et al., 2018b), suggested that the plasters, with the possible exception of sample 51A, dated at least from the early Xolalpan phase or later (AD 350), when incorporation of glass shards into the *enlucido* became widespread throughout Teotihuacan.

Plagioclase was the most abundant mineral in most samples, followed by quartz, biotite, opaque minerals and calcite (Table 2). Pyroxene (samples 5b, 53, 60C and 61A), amphibole (samples 5A, 5B, 51A, 52B, 60B and 61A) and olivine (samples 5B, 53, 60C and 61A) were also present.

Sample 61B differed from the others in exhibiting a clear prevalence of calcite over other minerals in the *enlucido*; numerous angular limestone fragments were evident in this sample, which were interpreted as most likely being unburned limestone (Fig. 4d). Other unburned limestone fragments were visible in samples 52A and 52B, while lime lumps were present in all samples representing the remains of the original limestone in the mixture (Table 2). The mean size of the *enlucido* aggregate in all samples was very small, and using the definitions of Wentworth (1992) varied from 'very fine sand' (sample 5B), to 'fine sand' for the remaining samples (Table 2).

The mean size of the *firme* aggregate was always greater than that of the *enlucido* (Table 2); it varied from 'granule' in most samples, to 'pebble', in sample 53. Some plasters, from samples 52B, 60B and 61A in particular, showed slight degrees of calcite re-crystallisation. All samples had more binder in the *enlucido* than aggregate (Table 2), and in general, the binder / aggregate ratio in this layer was approximately 1.5 in samples 51A, 52A and 61B, approximately 2.4 in samples 5A, 5B and 52B, and between 3 and 5, in samples 53, 60B, 60C, 61A and 61C. In the samples that still had a *firme* layer, the binder / aggregate ratio was between 0.6 and 1.

The presence of fragments of reused plaster --- particularly *enlucido* with glass shards --- in sample 5B, inside the *firme* layer, was very interesting (Fig. 4e and 4f). The pre-Columbian practice of reusing existing building materials, plaster in particular, was highlighted by Barba et al. (2009), referring to plasters from Teotihuacan, and by Miriello et al. (2011), with reference to the plasters of the Templo Mayor of Tenochtitlan (Mexico City). Here, we conceived that sample 5B belonged to a wall / floor that had at least two phases in which glass shards were incorporated, as it was possible to see these glass shards in not only the *enlucido* layer but also the reused plaster.

The presence of ancient mortars and plasters, reused as aggregate, inside new mortars or plasters allowed us to form an interesting hypothesis, which was linked to the high seismicity level of the study area. This has been evidenced and confirmed from other parts of the world, such as Pompeii (Italy), for example (Miriello et al., 2018a). In fact, in the archaeological area of Pompeii, all mortars belonging to the construction phase that followed the 62 AD earthquake incorporated fragments of mortars and plasters recycled from earthquake-damaged buildings (Miriello et al., 2018a, 2018b). This construction feature has turned ancient mortars and plasters into powerful evidence for the occurrence of ancient earthquakes. In the case of pre-Columbian buildings, we still do not have enough data to confirm the hypothesis that the re-use of mortars and plasters was related to ancient earthquakes, although it is clear that both Mexico City and Teotihuacan are located in seismic areas. We hope that it will be possible to confirm this hypothesis with further research, in which archaeological, historical, and mortar and plaster compositional data can be combined.

In general, it was interesting to observe that the study of the plasters revealed some differences between samples. For example, sample 51A, from the Plaza de las Columnas, was different to the others, in that it did not display abundant glass shards, while there were numerous angular limestone fragments in sample 61C (Techinantitla). These have been interpreted as unburned limestone, and other unburned limestone fragments were found in samples 52A and 52B from the Plaza de las Columnas. These data indicated that, although the samples were not recovered *in-situ*, it was feasible that the two compounds had different construction phases, were built by different groups of workers—as the archaeological excavations carried out at the Techinantitla site have confirmed (De la Fuente, 1996)—or perhaps that there was inadequate production control of lime at the Tula outcrops.

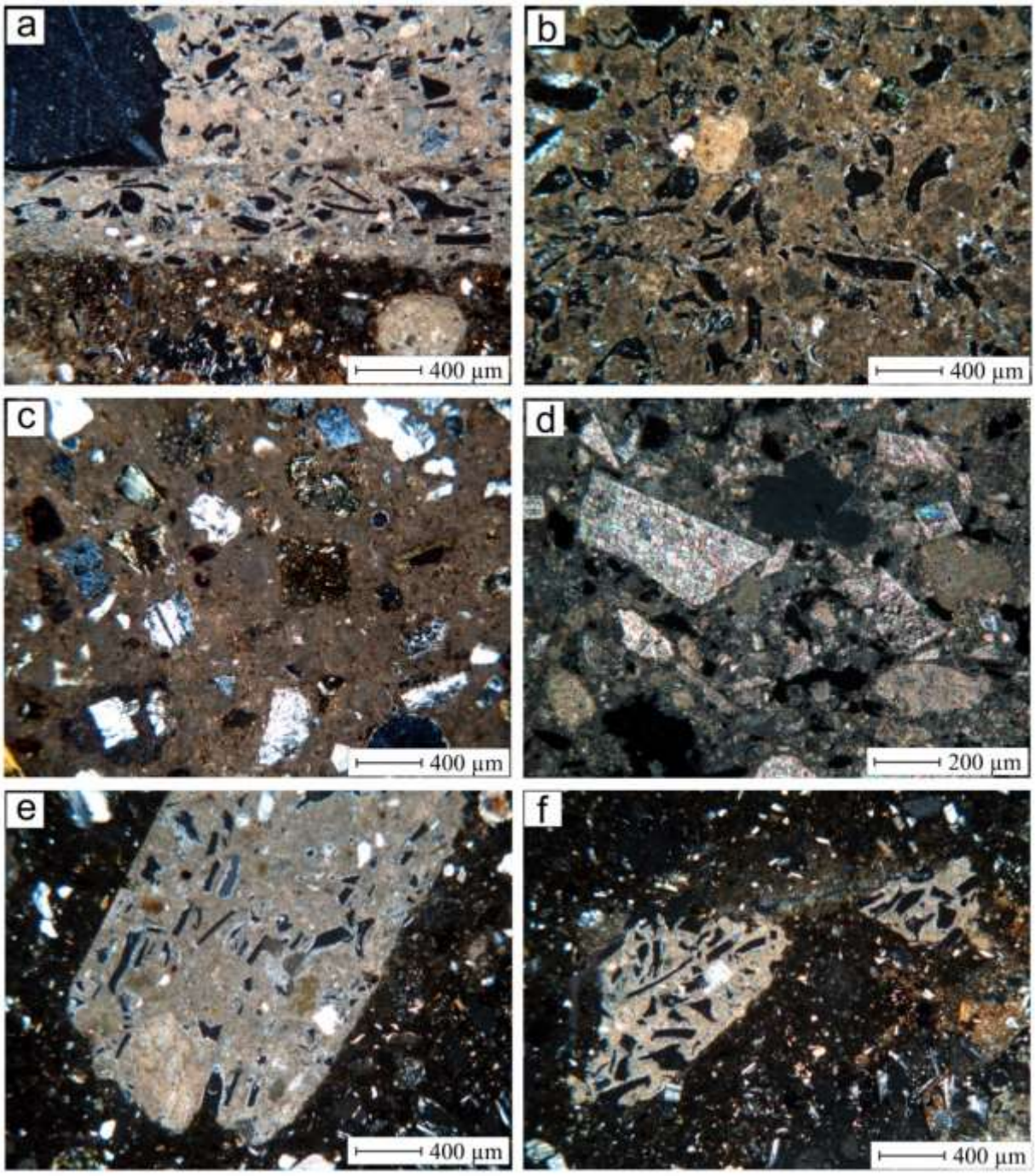

Fig. 4. Microphotographs in thin section, using optical microscopy under crossed nicol, with details of the plaster samples: **a)** Two *enlucido* layers and a *firme* layer in sample 5B; **b)** An *enlucido* layer showing glass shards from sample 5A; **c)** An *enlucido* layer with traces of glass shards, volcanic fragments, and mineralogical phases such as quartz and plagioclase from sample 51A; **d)** Unburned limestone in sample 61C; **e)** and **f)** Fragments of recycled *enlucido* in the sample 5B *firme* layer.

Sample	Layer	Max. aggregate size (mm)	Mean aggregate size (mm)	Wenthoworth size	Mean Roundnes	Sorting	Mineralogical phases	Glass shard	Other Volcanic fragments (Tezontle)	Other	%A	%B	%MP
5A	*Enlucido*	0.86	0.37	Fine sand	VA -LS	WS	Pl, Qzt, Cal, Amp, Om	***	*	Lime lumps	30	69	1
5B	*Enlucido (2 layers)*	0.50	0.20	Very fine sand	SA - LS	WS	Pl. Amp, Qzt, Cal, Om	***	*	Lime lumps	30	67.5	2,5
	Firme	7.50	3.60	Granule	SR - HS	PS	Pl, Px, Ol, Bt, Qtz, Om	-	***	Fragments of reused enlucido with glass shards	48	37	15
51A	*Enlucido*	1.00	0.23	Fine sand	A -LS	PS	Pl, Qzt, Amp, Bt, Om	*	***	Lime lumps	40	52.5	7.5
52A	*Enlucido*	0.92	0.19	Fine sand	VA - LS	WS	Pl, Qtz, Om	**	**	Lime lumps, unburned limestone	35	55	10
52B	*Enlucido*	2.00	0.20	Fine sand	VA - LS	PS	Pl, Qzt, Bt, Amp, Cal, Om	***	*	Lime lumps, unburned limestone, recristallizzed calcite	25	65	10
53	*Enlucido (2 layers)*	0.86	0.23	Fine sand	VA -LS	MS	Pl, Om, Qzt, Cal, Bt	***	**	Lime lumps	20	75	5
	Firme	7.00	4.50	Pebble	SR - HS	PS	Pl, Px, Ol, Qzt, Om	-	***	-	46	39	15
60B	*Enlucido*	0.78	0.24	Fine sand	VA - LS	WS	Pl, Qzt, Amp, Om	***	*	Lime lumps, recristallized calcite	18	80	2
60C	*Enlucido*	1.02	0.22	Fine sand	A -LS	WS	Pl, Qzt, Cal, Om	***	*	Lime lumps	20	78	2
	Firme	8.00	3.20	Granule	SR - HS	PS	Pl, Px, Qzt, Cal, Bt, Ol, Om	-	***	-	40	42	18
61A	*Enlucido (2 layers)*	0.62	0.22	Fine sand	SA - LS	WS	Pl, Qzt, Om, Cal, Amp	***	*	Lime lumps, recristallized calcite	15	82	3
	Firme	11.00	4.00	Granule	SR - HS	PS	Pl, Px, Qzt, Bt, Ol, Om	-	***	-	48	32	20
61B	*Enlucido*	1.02	0.35	Medium sand	SA - LS	WS	Cal, Pl, Qzt, Bt, Om	***	*	Lime lumps	35	62.5	2.5
61C	*Enlucido*	0.80	0.26	Coarse sand	VA - LS	WS	Cal, Pl, Qzt, Om	***	*	Lime lumps, unburned limestone	20	78.5	1.5

Table 2. Petrographic features of plaster sample thin sections [Roundness legend (after Boggs, 2010)—A: angular; SA: sub-angular; SR: sub-rounded; HS: high sphericity; LS: low sphericity. Sorting legend (after Jerram, 2001; Boggs, 2010)—MS: moderately sorted; WS: well sorted; PS: poorly sorted. Mineralogical phases—Amp: amphibole; Bt: biotite; Ol: olivine; Om: opaque minerals; Pl: plagioclase; Px: pyroxene; Qtz: quartz. ***: abundant; **: medium; *: traces; - : absent]. Semi-quantitative aggregate (A), binder (B) and macroporosity (MP) estimations were performed with the aid of comparative visual charts (Ricci Lucchi, 1980; Best, 2003).

3.2. Pigments

The p-XRF technique has been frequently used to obtain information on the elemental compositions of cultural heritage artefact surfaces (Potts and West, 2008; Shugar and Mass, 2014). For murals, the presence of particular chemical elements or their combinations has allowed authors to hypothesise on the use of

particular mineral pigments (Moioli and Seccaroni, 2000; Seccaroni and Moioli, 2000; Miriello et al., 2018b). The p-XRF technique was applied to painted areas of samples 52A, 60B, 60C and 61 A (Fig. 5), with the results, as summarized in Fig. 6, showing that red areas were characterized by a significant Fe presence, green areas had a significant Cu presence and non-pigmented areas mainly showed high Ca content. These data indicated that red coloration was most likely due to the use of iron oxides, such as hematite (Fe_2O_3), while green was presumably sourced from minerals containing copper (Cu), with malachite ($CuCO_3{\cdot}Cu(OH)_2$) being the most likely candidate. These pigments were spread on a base of lime; in fact, the non-pigmented areas have a high calcium (Ca) content. As reported in the literature, both malachite (green) and hematite (red) were part of the range of pigments used by Teotihuacan artists to create wall mural paintings (De la Fuente, 1996; Martínez García, 2012; López Puértolas et al., 2020). While red pigments have been found both on the floors and walls of Teotihuacan compounds, there have not been any reports of green being applied to floors.

Apart from its use in murals, red was also the most common colour used to paint large pyramids as well as the floors of some of the associated plazas. This information allowed us to identify the provenance of the analysed plaster fragments better, suggesting that samples displaying green had most likely come from compound walls.

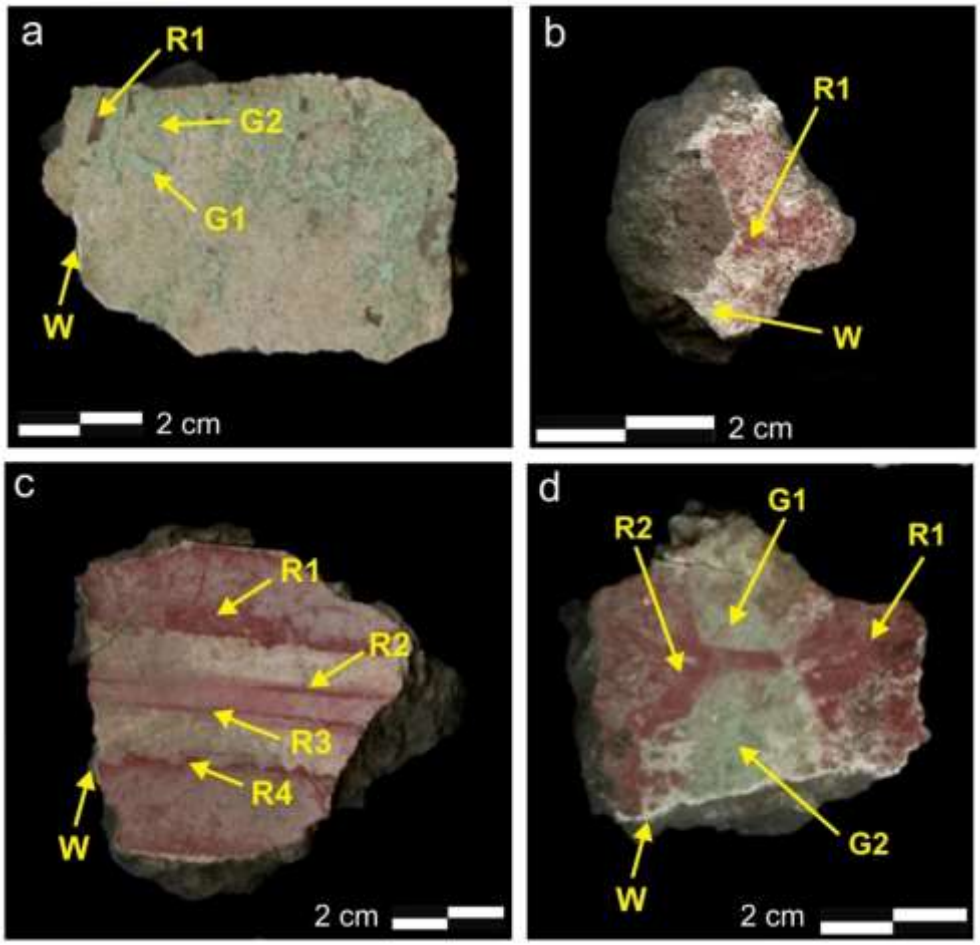

Fig. 5. Samples analysed by portable X-ray fluorescence (p-XRF) showing the analysis points [R = red; G = green; W = unpigmented plaster]: **a)** Sample 60B; **b)** Sample 52A; **c)** Sample 60C; **d)** Sample 61A.

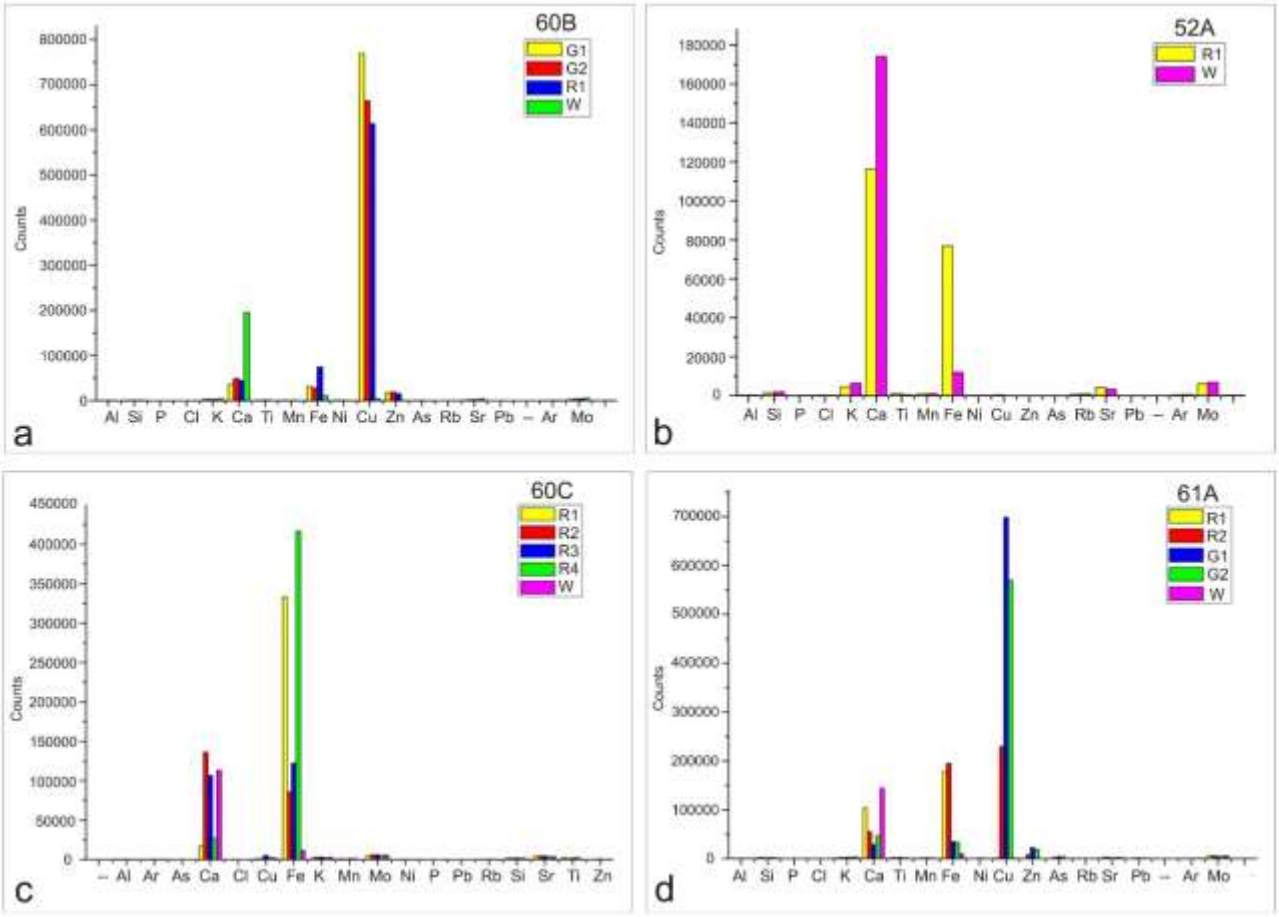

Fig. 6. X-ray intensities for the detected elements using p-XRF. Mo corresponds to the X-ray tube, and Ar to the air contribution [R = red; G = green; W= unpigmented plaster]: **a)** Sample 60B; **b)** Sample 52A; **c)** Sample 60C; **d)** Sample 61A.

3.3. Plaster hydraulicity

Volcanic materials used to make lime plasters could theoretically react with lime, producing C-S-H compounds, which are typical hydraulicity markers. On one side of the layer boundary, we see the glass shards that are present in the *enlucido* layer, and on the other, the so-called *tezontle* is used in both the *enlucido* and *firme*. The glass shards that formed the aggregate of the Teotihuacan plaster *enlucido* have been reported as having a rhyolitic composition (Barba et al., 2009; Barca et al., 2013; Pecci et al., 2018a), while the *tezontle* is a mix of scoriaceous volcanic rock, which is widely present and commonly used in Central Mexico. It has a variable composition, from basaltic trachyandesite to trachyandesite, as has been shown in the study of the mortars and plasters from the Templo Mayor of Tenochtitlan in Mexico City (Miriello et al., 2011, 2015), and it is likely that the *tezontle* in the Teotihuacan valley has the same composition.

To understand the hardness of the plasters, microhardness analyses were carried out on all *enlucido* samples in which the binder was composed exclusively of lime. The most likely hypothesis was that glass shards had the highest microhardness values, and reaction with lime might provide intermediate values. The results of

the analyses have been summarized in Table 3 and Fig. 7, where it can be seen that the highest mean Vickers microhardness values were found in samples 51A, 52A and 60C, with the maximum mean value found in 60C.

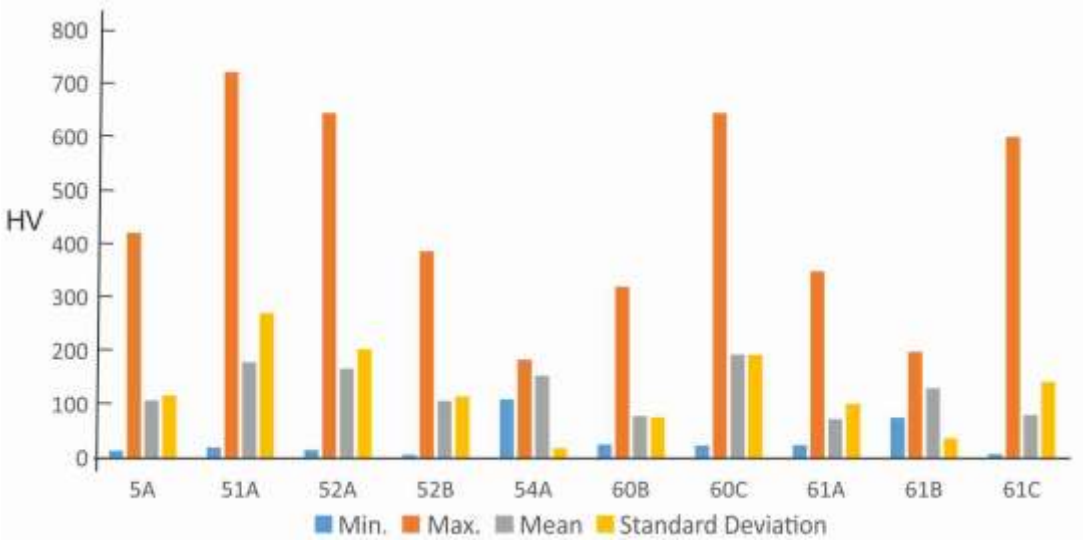

Fig. 7. Results from Vickers microhardness measurements performed on plaster *enlucido* layers.

Measure	Sample								
	5A	**51A**	**52A**	**52B**	**60B**	**60C**	**61A**	**61B**	**61C**
1	14.43	34.79	74.45	7.06	26.41	101.13	35.38	85.69	36.94
2	59.64	31.51	112.14	49.84	34.50	58.35	35.68	83.47	55.88
3	94.23	22.92	26.41	338.28	36.94	24.40	33.92	199.36	26.61
4	32.82	24.75	32.29	44.31	30.77	46.95	31.51	142.74	96.90
5	80.29	40.01	32.03	72.65	195.38	112.14	32.65	129.15	140.33
6	422.56	41.88	645.92	34.79	26.02	477.03	30.70	153.02	51.39
7	43.07	115.62	477.03	98.28	60.30	139.24	31.58	140.33	43.47
8	72.65	46.04	112.14	387.61	98.29	645.92	29.35	184.18	52.46
9	30.77	722.60	85.69	264.19	50.86	77.29	316.17	117.42	7.78
10	63.08	37.59	55.28	46.49	320.92	435.27	33.36	184.18	17.00
11	270.44	722.60	580.83	43.47	28.25	75.38	63.53	137.98	18.61
12	28.90	20.46	56.48	44.73	68.07	58.99	24.92	133.46	17.31
13	307.73	62.37	16.04	105.64	52.69	99.69	24.57	121.14	18.05
14	50.65	722.60	121.14	26.80	63.80	104.10	349.69	76.32	37.59
15	57.07	56.48	98.28	46.49	101.13	462.47	41.49	82.39	601.39
Average	108.56	180.15	168.41	107.38	79.62	194.56	74.30	131.39	81.45

Table 3. Microhardness measurements expressed in HV (Vickers Scale); 15 measurements were carried out on each sample and then averaged to establish the final result.

However, crossing petrographic data (Table 2) with these microhardness values (Table 3) did not reveal any correlation between high glass shard content and high levels of microhardness, except for sample 60C. In fact, sample 51A, which had a low glass shards content, also had a very high level of microhardness. These observations suggested that it was not the glass shards that developed plaster hydraulicity (also referred to as pozzolanic) reactions. To understand this problem better and to highlight any reaction between the volcanic materials and the binder, a microchemical approach was adopted (Miriello et al., 2010; Raneri et al., 2018). In Fig. 8 we have plotted the EDS microchemical map of a glass shard in sample 5A, and it can be seen quite clearly that there is no reaction rim around the glass shard because the Si and Al concentrations remain constant throughout the binder without increasing near the glass shard inside the *enlucido*.

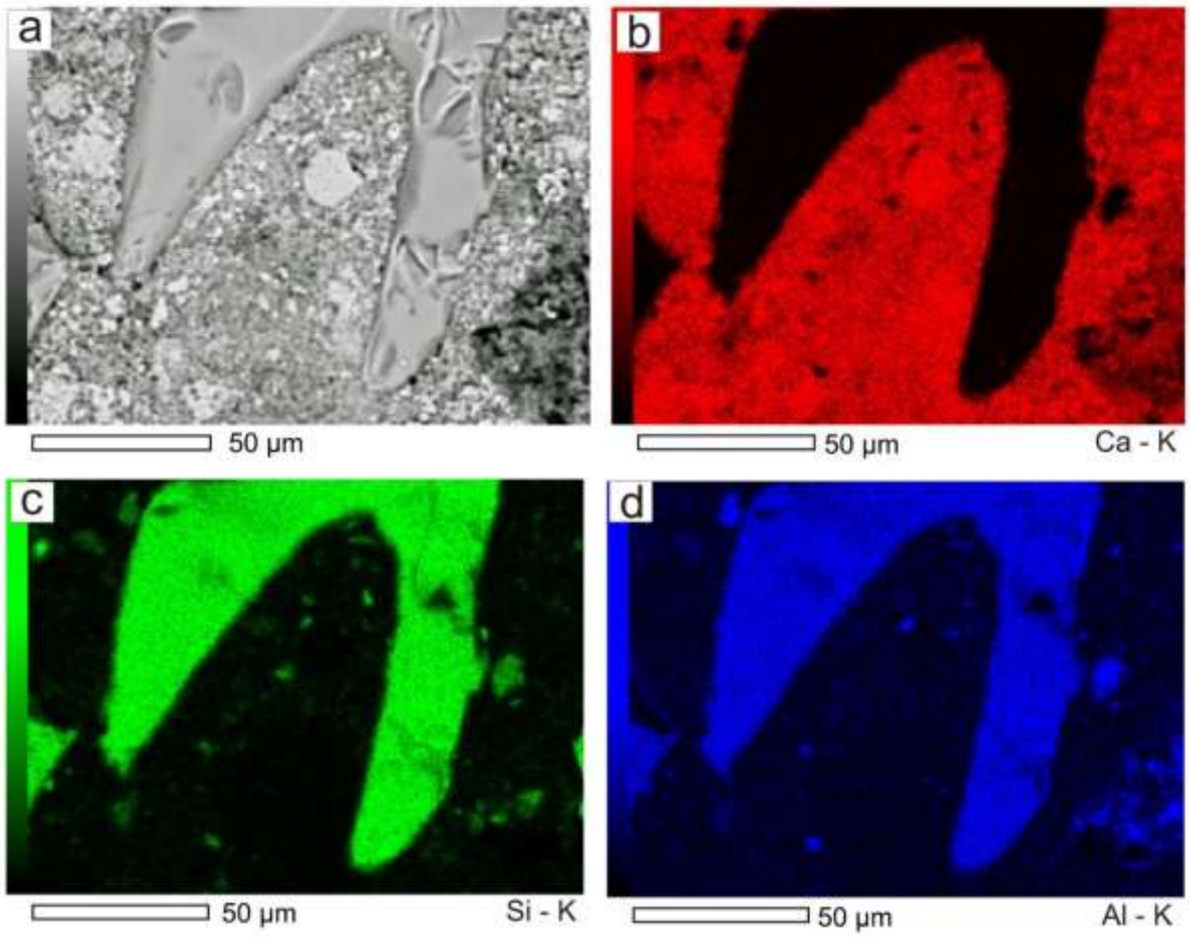

Fig. 8. a) EDS image with glass shard detail from sample 5A. EDS micro-chemical maps showing **b)** Ca-K content; **c)** Si-K content; **d)** Al-K content.

It was then surmised that the *tezontle* presence in the samples could provide an alternative explanation for plaster hydraulicity—although this idea seemed somewhat counter-intuitive, as most of the *tezontle* was found in the innermost layer of the plaster, the *firme*, and not in the *enlucido* layer.

To look into this more thoroughly, an EDS microchemical map of a *tezontle* fragment in the sample 51A *enlucido* was prepared (Fig. 9c). In contrast to the results from the glass shard analysis, this EDS microchemical map clearly showed the presence of a reaction rim around the *tezontle* fragment, confirmed by the increase in Si concentration near the *tezontle* fragment. These initial microchemical observations showed that *tezontle* was much more reactive than glass shards, even when both of them had enough Si.

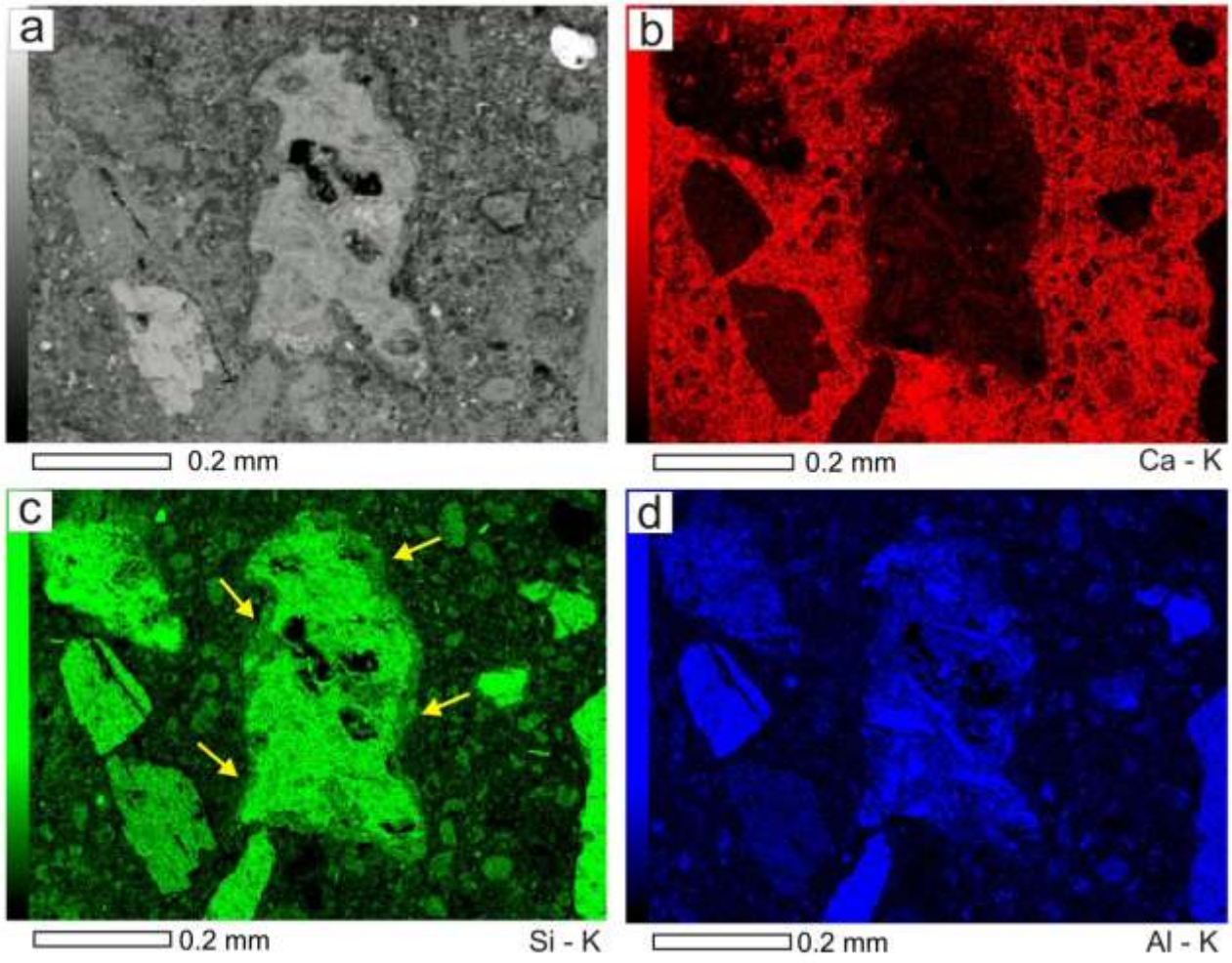

Fig. 9. a) EDS image showing *tezontle* fragment detail from sample 51A. EDS micro-chemical maps showing **b)** Ca-K content; **c)** Si-K content (yellow arrows indicate the reaction rim); **d)** Al-K content.

To confirm this hypothesis, we also measured the hydraulicity index (HI) of the sample 5A binder, where there are many glass shards, and of sample 51A, where there are many *tezontle* fragments, using the Vicat approach (Bonyton, 1966). The results showed that the HI of sample 5A binder was approximately 0.01 (Table 4), confirming that the glass shards did not produce any hydraulicization reactions—and that the lime was

an aerial type. In contrast, the sample 51A binder, with its many *tezontle* fragments, produced an HI range of 0.48–0.49 (Table 4), showing that the lime was a hydraulic type (Bonyton, 1966). These observations clearly demonstrated that it was the *tezontle,* and not the glass shards, which introduced the hydraulicity into the *enlucido* binder.

Enlucido content	Sample	SiO_2	TiO_2	Al_2O_3	Fe_2O_3	MgO	CaO	Na_2O	K_2O	P_2O_5	SUM	H.I.
Prevalence of glass shard	5A_B1	0.66	0.02	0.25	0.21	0.44	97.30	0.17	0.22	0.73	100.00	0.01
	5A_B2	0.35	udl	0.35	0.22	0.41	97.79	0.15	0.16	0.57	100.00	0.01
	5A_B3	0.45	udl	0.30	0.14	0.72	97.50	0.04	0.23	0.62	100.00	0.01
	5A_B4	0.41	udl	0.33	0.06	0.52	97.78	0.11	0.18	0.61	100.00	0.01
	5A_B5	0.59	0.02	0.26	0.07	0.53	97.73	0.10	0.22	0.48	100.00	0.01
	5A_B6	0.54	0.27	0.20	0.22	0.46	97.45	0.15	0.28	0.43	100.00	0.01
Prevalence of *tezontle*	51A_B1	24.27	0.22	6.30	1.15	0.74	65.82	0.21	0.76	0.53	100.00	0.48
	51A_B2	26.01	0.28	6.77	1.54	0.92	63.00	0.25	0.78	0.45	100.00	0.54
	51A_B3	30.03	0.56	9.73	3.47	1.46	53.09	0.46	0.74	0.47	100.00	0.79
	51A_B4	33.04	0.41	7.71	2.28	1.18	53.49	0.50	0.97	0.43	100.00	0.79
	51A_B5	24.87	0.23	5.07	0.71	0.71	67.43	0.17	0.61	0.20	100.00	0.45
	51A_B6	28.30	0.20	5.93	1.02	0.93	62.26	0.29	0.78	0.28	100.00	0.56

Table 4. EDS microanalyses performed on the *enlucido of* sample 5A, which mainly contained glass shards, and sample 51A, which mainly contained *tezontle*. Values are expressed in %wt [udl: under detection limit; H.I.: hydraulicity index].

It remained to be clarified, however, that if this was the case, just how the sample 60C *enlucido* exhibited such high levels of microhardness (Fig. 7), given that it contained very little *tezontle*. The explanation could involve the concept that the elements Si, Al, and Fe migrate from the *tezontle*, which in this case was present in a high amount in the *firme* layer, towards the *enlucido* layer.

To test this hypothesis, sample 61A, which had a very well preserved *enlucido*, was subjected to detailed EDS microchemical analysis. Two series of points were analysed (Fig. 10a). The first series (square symbols in the figure) was sampled from the more external part of the *enlucido*, while the second (triangular symbols) was sampled as close as possible to the *firme* layer (Fig. 10a). The results of this analysis can be seen in Figure 10b and Table 5, with the figure showing, very clearly that the binder closest to the *firme* had a higher Si, Al and Fe content than that measured in the upper part of the *enlucido*. This was definitive proof of the decisive role played by the *tezontle* present in the *firme* layer in converting the *enlucido* into a hydraulic material. This meant that it was no coincidence that the *enlucido* layer with the highest microhardness (sample 60C) was also the thinnest (Fig. 11), which meant that it could receive the chemical elements that produced hydraulicization reactions from the *tezontle* in the lower layer more easily.

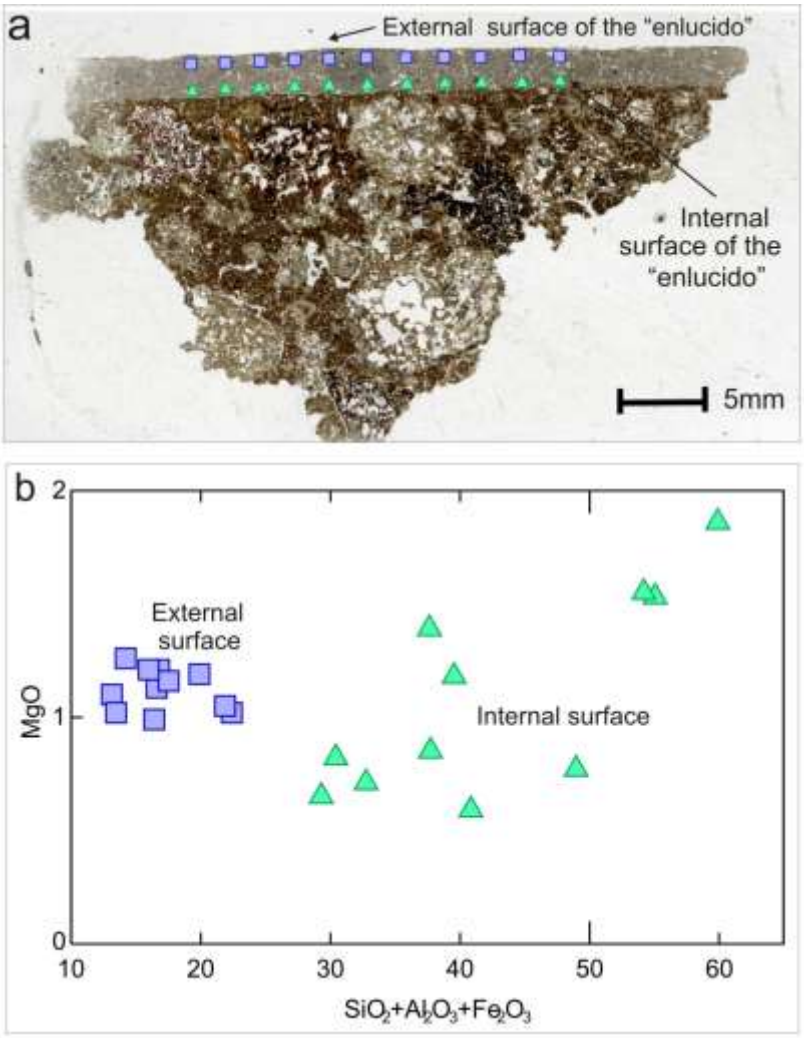

Fig. 10. a) Thin section from sample 61A under parallel nicol, showing the points analysed using EDS (squares represent points on the *enlucido* external surface; triangles represent points on the *enlucido* internal surface; **b)** Biplot diagram showing (SiO_2 + Al_2O_3 + Fe_2O_3) vs MgO.

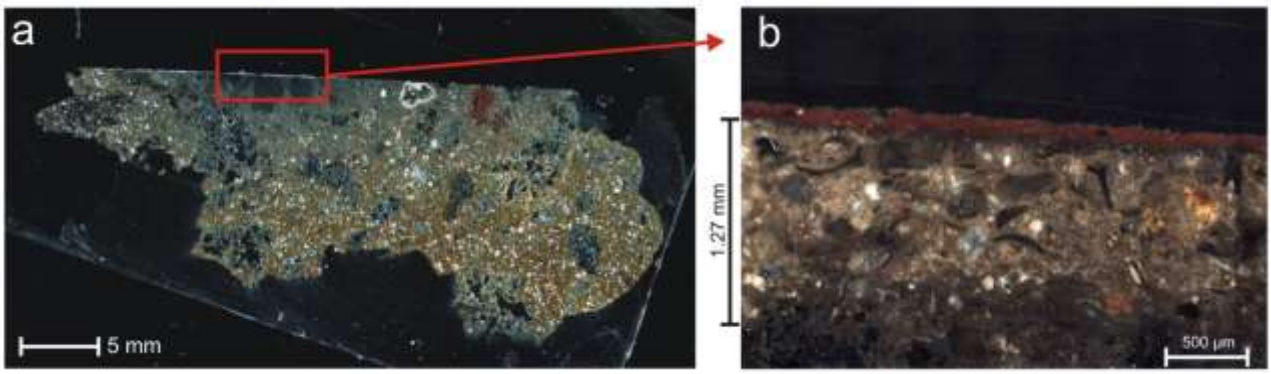

Fig. 11. a) Thin section from sample 60C under crossed nicol, with particular of the thin layer of *enlucido*; **b)** Image of the *enlucido* of sample 60C, in reflected light, where it is highlighted its thin thickness (1.27 mm).

Analyzed point	SiO_2	Al_2O_3	Fe_2O_3	MnO	MgO	CaO	Na_2O	K_2O	P_2O_5	SO_3	ClO	SUM
61A_B1_ex	10.13	5.69	0.77	udl	1.13	79.59	0.58	0.48	1.12	0.17	0.34	100
61A_B2_ex	8.79	3.62	0.72	0.41	1.10	82.23	0.62	0.57	0.93	0.22	0.51	100
61A_B3_ex	8.54	7.66	0.58	udl	1.21	79.08	0.90	0.55	0.57	0.15	0.76	100
61A_B4_ex	18.84	3.48	0.07	udl	1.02	73.20	0.61	1.03	0.91	0.28	0.55	100
61A_B5_ex	9.07	3.86	0.53	udl	1.02	82.11	0.93	0.59	0.98	0.30	0.62	100
61A_B6_ex	14.48	4.74	0.67	udl	1.19	75.38	0.80	0.61	1.15	0.21	0.77	100
61A_B7_ex	10.13	5.58	0.69	udl	0.99	79.25	1.11	0.49	0.91	0.16	0.68	100
61A_B8_ex	14.85	6.34	0.68	udl	1.05	73.18	1.32	0.80	0.90	0.13	0.74	100
61A_B9_ex	12.19	4.65	0.68	udl	1.16	78.78	0.44	0.47	1.03	0.22	0.37	100
61A_B10_ex	11.12	4.24	0.62	udl	1.21	79.33	1.20	0.69	0.65	0.13	0.84	100
61A_B11_ex	9.44	3.89	0.87	udl	1.26	81.38	0.45	0.61	1.35	0.21	0.55	100
61A_B1_in	24.63	7.15	0.97	udl	0.71	60.93	2.11	1.37	1.01	0.24	0.87	100
61A_B2_in	41.72	15.02	3.14	udl	1.86	33.82	0.72	1.73	1.39	0.36	0.24	100
61A_B3_in	20.44	9.11	0.87	udl	0.82	65.18	1.53	0.53	0.99	0.27	0.27	100
61A_B4_in	21.98	6.62	0.69	udl	0.65	66.30	1.33	1.09	0.74	0.22	0.39	100
61A_B5_in	29.79	7.00	0.93	udl	0.85	56.47	1.29	1.85	0.99	0.34	0.49	100
61A_B6_in	38.78	14.05	2.22	udl	1.53	39.57	1.45	0.80	1.19	0.20	0.21	100
61A_B7_in	38.67	13.37	2.13	udl	1.55	39.75	1.28	0.95	1.52	0.24	0.54	100
61A_B8_in	29.10	9.10	1.34	udl	1.18	54.29	1.24	2.20	1.01	0.17	0.39	100
61A_B9_in	35.52	12.22	1.22	udl	0.77	44.86	2.00	1.70	1.06	0.20	0.45	100
61A_B10_in	32.30	7.88	0.66	udl	0.59	53.23	1.97	1.83	0.86	0.23	0.44	100
61A_B11_in	25.11	11.12	1.41	udl	1.39	56.42	1.51	0.71	1.41	0.39	0.53	100

Table 5. EDS microanalysis performed on the *enlucido* of sample 61A from the more external part of the *enlucido* (_ex) and from the area as close as possible to the *firme* layer (_in). Values are expressed in %wt [udl: under detection limit].

4. Conclusions

Through the study described here, we were able to confirm that the plasters from the Techinantitla and Plaza de las Columnas compounds in Teotihuacan were made of lime mixed with glass shards with some crushed *tezontle* in specific cases, and that the *firme* was made of clay mixed with *tezontle*, like other mud plasters from Teotihuacan. With respect to the pigments used to paint these plasters, we showed that hematite was used for the red colouration and malachite for green, with these two colours part of the range of pigments used by the artists of Teotihuacan to create wall paintings (De la Fuente, 1996; López Puértolas et al., 2020). We also noted the presence of ancient mortars and plasters reused as aggregates inside new mortars and plasters. This practice, which has also been noted in other parts of the world with high seismicity (Miriello et al., 2018a), suggests that studying ancient mortars and plasters and the search for evidence of their reuse could be a powerful tool for revealing the occurrence of ancient earthquakes.

The main findings from this study allowed us to definitively clarify an issue that has been debated for some time—that Teotihuacan plasters are hydraulic—and to elucidate those compositional features which made them hydraulic. The microchemical approach combined with microhardness analyses and petrographic data

showed that it was the *tezontle* volcanic material which produced hydraulicization reactions. In contrast, the glass shards showed no chemical reactivity, and furthermore, much of the chemical reactivity was found to come from the *tezontle* content in the preparation layer of the plaster, the *firme*.

As a result, it is now possible to explain that Teotihuacans decided to use just a thin layer of lime plaster mixed with glass shards to finish the architectonic surfaces in the buildings and plazas of Teotihuacan. In addition to providing an important economy to counter using expensive materials coming from remote places after a high-energy pyrotechnological transformation, the lime masters realized, somehow, that the best performance of the lime plaster was in 3–4 mm layers, which facilitated those chemical reactions with the *tezontle* in the contact layer that warrantied the operational hydraulic behaviour of the lime plaster layer. We could also now assume that the glass shards played another role in the mixture, rather than producing hydraulicity, and that the mud mortar mixed with *tezontle* had an unexpected effect on the properties of the lime layer.

This constituted an important technological contribution, which made a large difference to lime use in the Maya area, and confirmed development of a unique technological style which took advantage of local geological resource, as well as using foreign materials.

Declaration of competing interest

The authors declare that they have no known competing financial interests or personal relationships that could appear to influence the work reported in this paper.

Acknowledgements

These research activities were carried out at the UNAM and at the UNICAL. In particular at the Laboratorio Nacional de Ciencias para la Investigación y Conservación del Patrimonio Cultural (LANCIC) - sede Instituto de Física, with support of grant numbers CONACYT LN293904, LN299076 and LN314846 as well as funding from PAPIIT UNAM grant IN112018, the Laboratorio de paleosuelos y taller de laminación, CENISA, the Instituto de Investigaciones Antropológicas, UNAM, and the "Laboratorio di Microscopia Elettronica e Microanalisi", UNICAL. This study also formed part of the ERAAUB research group work program (2017 SGR 1043). Part of this work was the result of a degree thesis developed in collaboration with UNICAL, UNAM, and the Universidad de Barcelona. The samples analysed in this work were collected as part of archaeological projects carried out by the UNAM. We thank the Consejo de Arqueología, INAH, for providing approval to study the samples (Oficio 401.1S.3-2020/1186).

The authors acknowledge the technical support at LANCIC, UNAM, provided by Alejandro Mitrani and Juan Gabriel Morales.

References

Barba, L., Blancas, J., Manzanilla, L.R., Ortiz, A., Barca, D., Crisci, G.M., Miriello, D., Pecci, A. 2009. Provenance of the limestone used in Teotihuacan (Mexico): A methodological approach. Archaeometry 51, 525-545.

Barba, L., Ortiz, A., Pecci, A. 2019. The innovations of Teopancazco: The flattened lime with volcanic glass. Arqueologia Mexicana 27, 39–42.

Barca, D., Miriello, D., Pecci, A., Barba, L., Ortiz, A., Manzanilla, L.R., Blancas, J., Crisci, G.M. 2013. Provenance of glass shards in archaeological lime plasters by LA-ICP-MS: Implications for the ancient routes from the Gulf of Mexico to Teotihuacan in Central Mexico. Journal of Archaeological Science 40, 3999–4008.

Barca, D., Pecci, A., Barba, L., Crisci, G.M., De Luca, R., Marabini, S., Manzanilla, L.R., Ortiz, A., Blancas, J., Pastrana, A., Miriello, D. 2019. Geochemical and petrographic characterization of pyroclastic deposits of Los Humeros Volcanic Complex used as aggregates in the plasters from Teotihuacan (Mexico). Microchemical Journal 145, 852–863.

Boggs, S.Jr. 2010. Petrology of sedimentary rocks, 2nd edn. Cambridge University Press, Cambridge.

Bonyton, R.S. 1966. Chemistry and Technology of Lime and Limestone. John Wiley & Sons, NewYork.

Cabrera, R. 1996. Amanalco. Barrio de las Pinturas Saqueadas. Techinantitla y Tlacuilapaxco, in De la Fuente, B. 1996. Pintura Mural Prehispanica en Mexico: Teotihuacan. UNAM, Mexico, 131–138

Cowgill, G. 2015. Ancient Teotihuacan. Early urbanism in Central Mexico. Cambridge University Press, New York.

De la Fuente, B. 1996. Pintura Mural Prehispanica en Mexico: Teotihuacan. UNAM, Mexico.

De Luca, R., Ontiveros, M.A.C., Miriello, D., Pecci, A., Le Pera, E., Bloise, A., Crisci, G.M. 2013. Archaeometric study of mortars and plasters from the Roman City of Pollentia (Mallorca - Balearic Islands). Periodico di Mineralogia 82, 353–379.

Jerram, D.A. 2001. Visual comparators for degree of grain-size sorting in two and three-dimensions. Computers & Geosciences 27, 485–492.

López Puértolas, C., Manzanilla-Naim, L., Vázquezde-Ágredos-Pascual, M.L. 2020. Characterization of color production in Xalla's palace complex, Teotihuacan. STAR: Science & Technology of Archaeological Research, 1–13.

Magaloni, D., 1996. El espacio pictórico teotihuacano. Tradición y técnica, in De la Fuente, B. 1996. Pintura Mural Prehispanica en Mexico: Teotihuacan. UNAM, Mexico, 187–225.

Manzanilla, L.R. 2009. Les palais et résidences de Teotihuacan, Les Dossiers d'Archéologie 17, 20–23.

Manzanilla, L.R. (ed.) 2012. Estudios arqueométricos del centro de barrio de Teopancazco en Teotihuacan, UNAM, Mexico.

Manzanilla, L.R. 2015 Cooperation and tensions in multiethnic corporate societies using Teotihuacan, CentralMexico, as a case study. PNAS 30:9141–9490.

Manzanilla, L. R. (ed.) 2018. Teopancazco como centro de barrio multiétnico de Teotihuacan. los sectores funcionales y el intercambio a larga distancia. Primera parte. Teopancazco y sus sectores Funcionales. Instituto de Investigaciones Antropológicas, Universidad Nacional Autónoma de México, México.

Marquina, I. 1922. Arquitectura y Escultura, in: M. Gamio (Ed.), La Población del Valle de Teotihuacan, Secretaría de Agricultura y Fomento, Mexico, 99–164.

Martínez García, C., Ruvalcaba Sil, J.L., Manzanilla Naim, L., Riquelme, F. 2012. Teopancazco y su pintura. Aplicación de técnicas analíticas PIXE, MEB.EDX, DRX, FTIR y Raman, in Manzanilla Naim (ed.)Estudios arqueométricos del centro de barrio de Teopancazco en Teotihuacan, UNAM, Mexico, 165–210.

Millon, R., 1973. Urbanization at Teotihuacan, Mexico. The TeotihuacanMap, University of Texas University Press, Austin.

Miriello, D., Barca, D., Bloise, A., Ciarallo, A., Crisci, G.M., De Rose, F., Gattuso, C., Gazineo, F., La Russa, M.F., 2010. Characterisation of archaeological mortars from Pompeii (Campania, Italy) and identification of construction phases by compositional data analysis. Journal of Archaeological Science 37, 2207–2223.

Miriello, D., Barca, D., Crisci G.M., Barba, L., Blancas, J., Ortiz, A., Pecci, A., Lopez Luján, L. 2011. Characterization and provenance of lime plasters from the Templo Mayor of Tenochtitlan (Mexico City). Archaeometry 53, 1119–1141.

Miriello, D., Lezzerini, M., Chiaravalloti, F., Bloise, A., Apollaro, C., Crisci, G.M. 2013. Replicating the chemical composition of the binder for restoration of historic mortars as an optimization problem. Computers and Concrete 12, 553–563.

Miriello, D., Barca, D., Pecci, A., De Luca, R., Crisci, G.M., López, L.L., Barba, L. 2015. Plasters from different buildings of the Sacred Precinct of Tenochtitlan (Mexico City): characterization and provenance. Archaeometry 57, 100–127.

Miriello, D., Barba, L., Blancas, G., Bloise, A., Cappa, M., Cura, M., De Angelis, D., De Luca, R., Pecci, A., Taranto, M., Yavuz, H.B., Crisci, G.M. 2017. New compositional data on ancient mortars from Hagia Sophia (Istanbul, Turkey). Archaeological and Anthropological Sciences 9, 499–514.

Miriello, D., Bloise, A., Crisci, G.M., De Luca, R., De Nigris, B., Martellone, A., Osanna, M., Pace, R., Pecci, A., Ruggieri, N. 2018a. New compositional data on ancient mortars and plasters from Pompeii (Campania – Southern Italy): Archaeometric results and considerations about their time evolution. Materials Characterization 146, 189–203.

Miriello, D., Bloise, A., Crisci, G.M., De Luca, R., De Nigris, B., Martellone, A., Osanna, M., Pace, R., Pecci, A., Ruggieri, N. 2018b. Non-Destructive Multi-Analytical Approach to Study the Pigments of Wall Painting Fragments Reused in Mortars from the Archaeological Site of Pompeii (Italy). Minerals 8, 134.

Moioli, P.; Seccaroni, C. 2000. Analysis of art objects using a portable X-ray fluorescence spectrometer. X-ray Spectrometry 29, 48–52.

Myron Best, G. 2003. Igneous and metamorphic petrology, 2nd edn. Blackwell, Oxford.

Muñoz Fuentes, M. 2019. La integración de la pintura mural de Techinantitla y Tlacuilapaxco, barrio de Amanalco a la plástica Teotihuacana. Tesis de doctorado. Programa de Posgrado en Historia del Arte, UNAM.

Murakami, T. 2010. Power Relations and Urban Landscape Formation: A Study of Construction Labor and Resources at Teotihuacan (Unpublished PhD thesis), Arizona State University.

Murakami, T. 2016. Materiality, regimes of value, and the politics of craft production, exchange, and consumption: a case of lime plaster at Teotihuacan, Mexico. Journal of Archaeological and Anthropological Sciences 42, 56–78.

Pecci, A., Miriello, D., Barca, D., Crisci, G.M., De Luca, R., Ortiz, A., Manzanilla, L.R., Blancas, J., Barba, L. 2018a. Identifying a technological style in the making of lime plasters at Teopancazco (Teotihuacan, México). Journal of Archaeological and Anthropological Sciences 10, 315–335.

Pecci, A., Miriello, D., Barca, D., Crisci, G.M., De Luca, R., Ortiz, A., Manzanilla, L.R., Blancas, J., Barba, L. 2018b. Estudios arqueométricos de mezclas de cal en Teopancazco: caracterización, procedencia de las materias primas y definición de un estilo tecnológico, Manzanilla L. R. (ed.) Teopancazco como centro de barrio multiétnico de Teotihuacan. los sectores funcionales y el intercambio a larga distancia. Primera parte. Teopancazco y sus sectores Funcionales. Instituto de Investigaciones Antropológicas, Universidad Nacional Autónoma de México, México, 585-619. ISBN 978-607-30-1113-6.

Potts, P.J., West M., 2008. Portable X-ray Fluorescence Spectrometry, Capabilities for In Situ Analysis. The Royal Society of Chemistry, London.

Raneri, S., Pagnotta, S., Lezzerini, M., Legnaioli, S., Palleschi, V., Columbu, S., Neri, N.F., Mazzoleni, P. 2018. Examining the reactivity of volcanic ash in ancient mortars by using a micro-chemical approach. Mediterranean Archaeology and Archaeometry 18, 147–157.

Ricci Lucchi, F. 1980. Sedimentologia Parte I: Materiali e tessiture dei sedimenti. Clueb, Bologna.

Ruvalcaba, J.L., Ramírez Miranda, D., Aguilar Melo, V., Picazo, F. 2010. SANDRA: a portable XRF system for the study of Mexican cultural heritage. X-Ray Spectrometry 39, 338–345.

Seccaroni, C., Moioli, P. 2000. Fluorescenza, X. Prontuario per L'analisi XRF Portatile Applicata a Superfici Policrome; Nardini Editore: Firenze, Italy, 2001.

Shugar, A.N., Mass J.L., 2014. Handheld XRF for Art and Archaeology (Studies in Archaeological Sciences), Leuven University Press, Leuven.

Taylor, H.F.W 1997 Cement chemistry, 2nd edn. Thomas Telford, London, 113–128.

Villaseñor, I., Cuevas García, M., Barba, L., 2009. Indicadores de actividad ritual en los templos del Grupo de las Cruces de Palenque, Chiapas, Memorias del XXII Simposio de Investigaciones Arqueológicas en Guatemala, Museo Nacional de Antropología y Etnología (21–26 de julio 2008), Ciudad de Guatemala.

Wentworth, C.K. (1922). A scale of grade and class terms for clastic sediments. *Journal of Geology*, 30, 377–392.